Available online at www.sciencedirect.com
SCIENCE DIRECT®
Chemical Physics Letters 374 (2003) 362–371
CHEMICAL PHYSICS LETTERS
www.elsevier.com/locate/cplett

Ultrafast heterodyne detected infrared multidimensional vibrational stimulated echo studies of hydrogen bond dynamics

John B. Asbury, Tobias Steinel, C. Stromberg, K.J. Gaffney, I.R. Piletic, Alexi Goun, M.D. Fayer *

Department of Chemistry, Stanford University, Stanford, CA 94305, USA

Received 19 February 2003; in final form 8 April 2003

Abstract

Multidimensional vibrational stimulated echo correlation spectra with full phase information are presented for the broad hydroxyl stretch band of methanol-OD oligomers in CCl_4 using ultrashort (<50 fs) infrared pulses. Hydrogen bond breaking permits data to be acquired for times much greater than the vibrational lifetime. The data indicates that vibrational relaxation leads to preferential hydrogen bond breaking for oligomers on the red side of the spectrum. An off diagonal peak in the correlation spectrum that appears at long time (>1 ps) shows that there is frequency correlation between the initially excited hydroxyl stretch and the frequency shifted hydroxyl stretch formed by hydrogen bond breaking.

1. Introduction

Hydrogen bonding liquids, such as alcohols and water, have complex structures and dynamics. Such liquids have generated a great deal of experimental [1–7] and theoretical [8–11] study because of their importance as solvents in chemical and biological systems. Recently, there have been major advances in understanding brought about by the application of ultrafast infrared experimental methods, particularly a variety of transient absorption experiments. The development of the ultrafast infrared vibrational echo technique [12–15], and the recent extension to multidimensional vibrational echo methods [16–18], provides a new approach for the study of condensed matter systems. Such techniques are beginning to be applied to hydrogen bonding systems [19].

Here we report the first application of ultrafast heterodyne detected multidimensional vibrational stimulated echoes with full phase resolution to the study of the dynamics of hydrogen bonding liquids. By using the shortest mid-IR pulses produced to date, (<50 fs or <4 cycles of light), it is possible to perform experiments on the entire broad hydroxyl stretching band of methanol-OD oligomers

* Corresponding author. Fax: 1-650-723-4817.
E-mail address: fayer@stanford.edu (M.D. Fayer).

0009-2614/03/$ - see front matter © 2003 Elsevier Science B.V. All rights reserved.
doi:10.1016/S0009-2614(03)00643-2

in carbon tetrachloride solution even though it is several hundreds of cm^{-1} wide. The spectrum includes both the 0–1 and 1–2 vibrational transitions. By using pulses that are transform limited in the sample and by controlling path lengths with accuracy of a small fraction of a wavelength of light along with proper data analysis, data are obtained with correct phase relationships across the entire spectrum. The proper phase relationships permit accurate separation of the absorptive and dispersive contributions to the spectrum. As a result, the 2D IR correlation spectra are obtained in a manner akin to 2D NMR spectroscopy [20,21].

The study of the vibrational dynamics of the hydroxyl stretching mode provides information on hydrogen bonds because of the strong influence hydrogen bonding has on the hydroxyl stretch frequency and dynamics [22]. For a methanol-OD (MeOD) in an oligomer, where the MeOD is both a hydrogen bond donor and acceptor (δ), the OD stretch is centered at ~2490 cm^{-1} and it has a FWHM of ~150 cm^{-1}. An MeOD that is a hydrogen bond donor but not an acceptor (γ) has a peak position of ~2600 cm^{-1} and a FWHM of ~80 cm^{-1}. An MeOD that is an acceptor but not a donor (β) has a spectrum centered at 2690 cm^{-1} with a 20 cm^{-1} FWHM [23,24]. The shift to the lower energy and the broad spectra of the δ and γ bands (see Fig. 1a) are caused by the change in the hydroxyl stretch potential with hydrogen bonding [23,24]. The high energy (blue) side of the δ band is thought to result from weaker hydrogen bonds and the low energy (red) side results from stronger hydrogen bonds [22]. Breaking a hydrogen bond changes the nature of the species and, therefore, its absorption frequency. In an oligomer longer than a trimer, if a δ breaks a hydrogen bond, two δ absorbers are lost from the absorption spectrum, and a γ and a β are formed [3]. Therefore, the dynamics of the hydroxyl stretch reflect the dynamics of the hydrogen bonds.

Fluctuations in the strengths of hydrogen bonds produces hydroxyl stretch vibrational dephasing and spectral diffusion [5,8,25]. Therefore, observation of vibrational dephasing provides information on the structural dynamics of hydrogen bonding networks. In general, direct spectroscopic

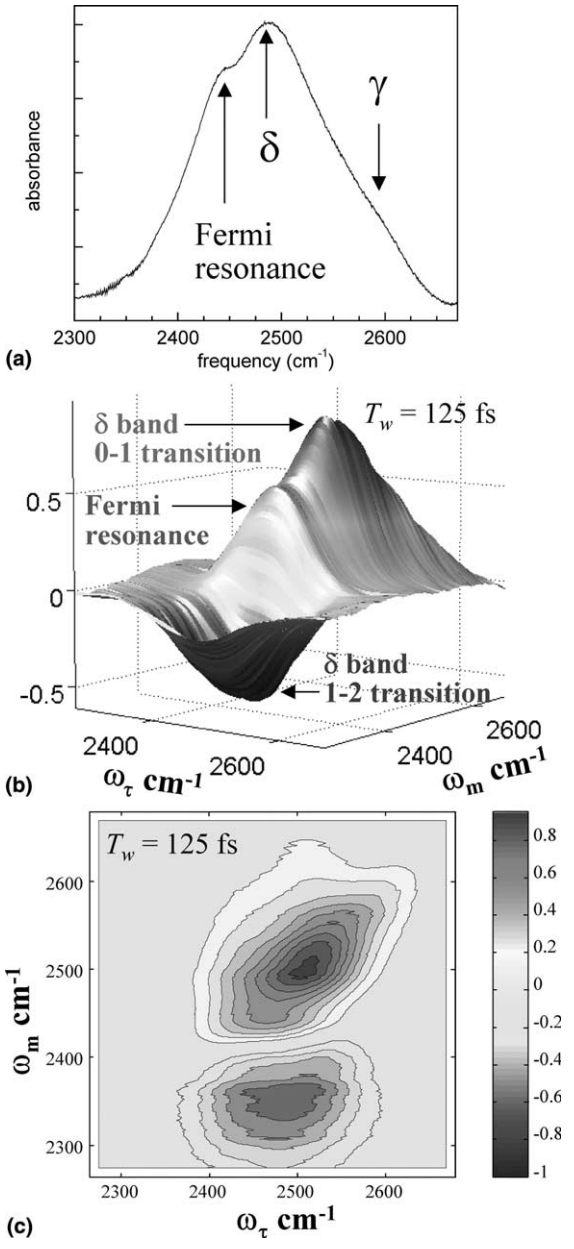

Fig. 1. (a) Linear absorption spectrum of OD stretching mode of methanol-OD in CCl_4. (b) The vibrational simulated echo correlation spectrum for $T_w = 125$ fs. The negative going peak in the foreground is from the 1–2 transition of the OD stretch. The positive going band is the 0–1 transition. The red edge of the positive going band arises from a Fermi resonance with the overtone of the methyl rocking mode. (c) A contour plot of the correlation spectrum for $T_w = 125$ fs. The red end of the positive going band has shape that is strongly influenced by the Fermi resonance.

observation of vibrational dephasing is prevented by the inhomogeneously broadened absorption lines observed in hydrogen bonded liquids. The inhomogeneous contribution to the line shape can be eliminated and the underlying dynamical line shapes can be observed using vibrational echo techniques [12–18,26]. Because of the complexity of hydrogen bonding systems like MeOD oligomers, separation of different contributions to the dynamical vibrational spectra require ultrafast multidimensional methods. Such methods can separate and narrow the dynamic spectral features [27], permitting the observation of distinct contributions to the dynamics.

2. Experimental procedures

The ultrashort IR pulses employed in the experiments are generated using a Ti:sapphire regeneratively amplified laser/OPA system. The output of the modified Spectra Physics regen is 26 fs transform limited 2/3 mJ pulses at 1 kHz rep rate. These are used to pump a substantially modified Spectra Physics short pulse IR OPA. The output of the OPA is compressed to produce <50 fs transform limited IR pulses as measured by collinear autocorrelation. For the experiments, the compression was readjusted to give transform limited pulses in the sample as measured by a sample that gave a purely non-resonant signal. The shot-to-shot IR stability is $\sim 1.0\%$, and the long-term stability is such that data were collected continuously for as long as 5 days.

The IR beam is split into five beams. Three of the beams are the excitation beams for the vibrational stimulated echo. A fourth beam is the local oscillator (LO) used to heterodyne detect the vibrational echo signal. One of the excitation beams is also used for pump–probe experiments, with the fifth beam as the probe beam in the pump–probe experiments. All of the beams that pass through the sample are optically identical and are compensated for GVD simultaneously. The vibrational echo signal combined with the LO is passed through a monochromator and detected by a 32 element MCT array. At each monochromator setting, the array detects 32 individual wavelengths. The sample, 10% MeOD in CCl_4, was held in a sample cell of CaF_2 flats with a spacing of 50 μm. The peak absorbance of the samples was 0.18. Such a low absorbance is necessary to prevent serious distortions of the pulses as they propagate through the sample.

The phase-resolved, heterodyne detected, stimulated vibrational echo was measured as a function of one frequency variable, ω_m, and two time variables, τ and T_w that are defined as the time between the first and second interactions and the second and third interactions, respectively. The measured signal is the absolute value squared of the sum of the vibrational echo electric field, S, and the local oscillator electric field, L: $|L+S|^2 = L^2 + 2LS + S^2$. The L^2 term is time-independent and the S^2 is very small; hence neither contributes to the time dependence of the signal. The spectrum of the $2LS$ term is the ω_m frequency axis. As the τ variable is scanned in 2 fs steps, the phase of the echo electric field is scanned relative to the fixed local oscillator electric field, resulting in an interferogram measured as a function of the τ variable. The interferogram contains the amplitude, sign, frequency, and phase of the vibrational echo electric field as it varies with τ. By Fourier transformation, this interferogram is converted into the frequency variable ω_τ.

The interferogram measured as a function of τ contains both the absorptive and dispersive components of the vibrational echo signal. However, two sets of quantum pathways can be measured independently by appropriate time ordering of the pulses in the experiment [21]. With pulses 1 and 2 at the time origin, pathway 1 or 2 is obtained by scanning pulse 1 or 2 to negative time, respectively. Adding the Fourier transforms of the interferograms from the two pathways, the dispersive component cancels leaving only the absorptive component. The 2D vibrational echo correlation spectra are constructed by plotting the amplitude of the absorptive component as a function of both ω_m and ω_τ.

Lack of perfect knowledge of the timing of the pulses and consideration of chirp on the vibrational echo pulse requires a 'phasing' procedure to be used. The projection slice theorem [20,21] is employed to generate the absorptive 2D correla-

tion spectrum. The projection of the absorptive 2D correlation spectrum onto the ω_m axis is equivalent to the IR pump–probe spectrum recorded at the same T_w, as long as all the contributions to the vibrational stimulated echo are absorptive. Consequently, comparison of the projected 2D vibrational stimulated echo spectrum to the pump–probe spectrum permits the correct isolation of the absorptive vibrational echo correlation spectrum from the 2D spectrum obtained from the addition of the two quantum pathways.

It is possible to come relatively close to the correct correlation spectrum prior to the 'phasing' procedure because the very short pulses permit their time origins to be known within a few fs. The frequency dependent phasing factor used to correct the 2D spectra has the form

$$\begin{aligned} S_C(\omega_m,\omega_\tau) &= S_1(\omega_m,\omega_\tau)\Phi_1(\omega_m,\omega_\tau) \\ &\quad + S_2(\omega_m,\omega_\tau)\Phi_2(\omega_m,\omega_\tau), \\ \Phi_1(\omega_m,\omega_\tau) &= \exp[i(\omega_m\Delta\tau_{LO,E} \\ &\quad + \omega_\tau\Delta\tau_{1,2} + \omega_m\omega_\tau C)], \\ \Phi_2(\omega_m,\omega_\tau) &= \exp[i(\omega_m\Delta\tau_{LO,E} \\ &\quad - \omega_\tau\Delta\tau_{1,2} + \omega_m\omega_\tau C)], \end{aligned} \tag{1}$$

S_C, is the correlation spectrum. S_1 and S_2 are the spectra recorded for pathways 1 and 2, respectively. $\Delta\tau_{LO,E}$ accounts for the lack of perfect knowledge of the time separation of the LO pulse and the vibrational echo pulse; $\Delta\tau_{1,2}$ accounts for the lack of perfect knowledge of the time origins of excitation pulses 1 and 2; and C accounts for the linear chirp caused by propagating of the vibrational echo through the sample. $\Delta\tau_{1,2}$ comes in with opposite sign for pathways 1 and 2. Following phasing, the errors in the time origins are $<100\times10^{-18}$ s and the chirp across the entire spectrum is $<200\times10^{-18}$ s. Full details of the experimental and data processing procedures will be presented subsequently.

3. Results and discussion

Figs. 1b and c are different presentations of the 2D correlation spectrum with $T_w = 125$ fs. For $T_w > 75$ fs, non-resonant contributions are negligible. The spectra are exclusively the absorptive component of the signal. The correlation spectrum has two distinct regions. The positive going band corresponds to the 0–1 transition of the δ band with some contribution from the 0–1 γ band on the blue edge. The large negative going band arises from the 1–2 transition of the δ band. As can be seen in the contour plot, the 1–2 band is off diagonal, located below the 0–1 band, because it is described by a three level rephasing diagram. The first interaction with the fields produces a 0–1 coherence at the 0–1 transition frequency that dephases. The second interaction yields a population in the $v = 1$ level, while the third interaction produces a 1–2 coherence that rephases and emits at the 1–2 transition frequency, which is shifted to the red by the anharmonicity ($\sim$100 cm^{-1}) [28].

In the linear absorption spectrum (Fig. 1a), a shoulder is clearly visible on the red side of the absorption spectrum. This shoulder has been assigned as an overtone transition of the methyl rocking mode (1232 cm^{-1}) [29], which gains oscillator strength through a Fermi resonance with the OD stretching mode. The red edge of the positive going 0–1 band in Fig. 1c is wider and has a different shape than the rest of the band. This region of the spectrum is dominated by the overtone transition at short T_w.

Fig. 2 shows the correlation spectrum of fully deuterated methanol (d-MeOD, CD_3-OD) for

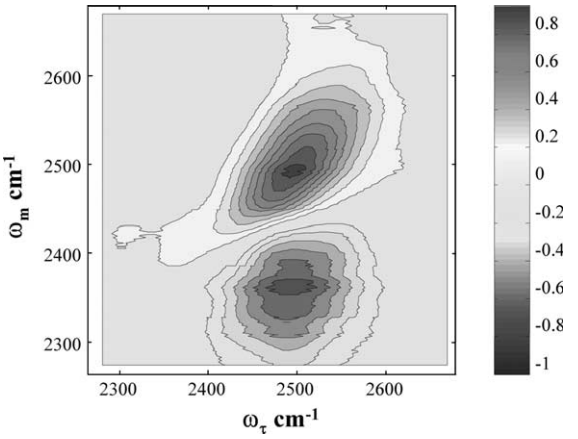

Fig. 2. The correlation spectrum for $T_w = 125$ fs taken on fully deuterated methanol (CD_3OD), which does not have the Fermi resonance. The distinctive shape on the red end of the positive going band seen in Fig. 1c is absent.

$T_w = 125$ fs, which should be compared to Fig. 1c that displays MeOD (CH_3-OD) data. In d-MeOD, the methyl rocking mode is shifted to substantially lower frequency, and there is no Fermi resonance between the overtone and the OD stretch. In the linear spectrum, the shoulder apparent in Fig. 1a is absent. As seen in Figs. 1c and 2, the correlation spectra are very different on the red part of the positive going 0–1 band. This portion of the MeOD spectrum is almost square in appearance and much broader than the corresponding portion of the d-MeOD. The shape arises because of the coupling between the methyl rock overtone and the OD stretching mode. The coupling generates off-diagonal peaks that produce the square shape. The coupling is confirmed by the change in the OD stretch lifetime when the methyl group is deuterated. In MeOD, the lifetime is ~400 fs, while in d-MeOD, it is ~1 ps. In MeOD, coupling to the overtone provides an efficient pathway for vibrational relaxation of the OD stretch [30]. When this pathway is removed because the CD_3 rock overtone is shifted to substantially lower energy, the remaining relaxation pathways are less efficient, and the lifetime lengthens.

Fig. 3 along with Fig. 1c show five contour plots at $T_w = 125$ fs, 450 fs, 1.2 ps, 1.8 ps, and 5.0 ps for MeOD. At 125 fs (Fig. 1c), the spectrum is dominated by the 0–1 band (positive) and the 1–2 band (negative). In the 450 fs plot, the negative going 1–2 band is less intense, and the 0–1 band is beginning to change shape. The vibrational lifetime

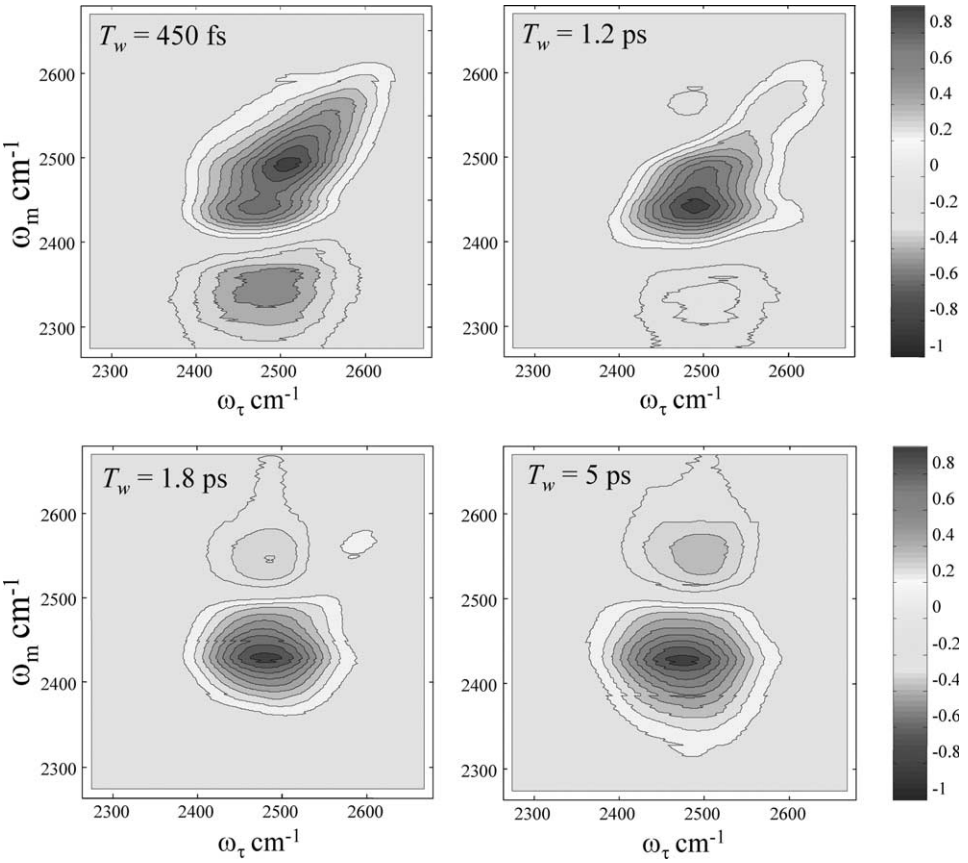

Fig. 3. Contour plots of the correlation spectra for $T_w = 450$ fs, 1.2, 1.8, and 5 ps. As T_w increases, the off-diagonal negative going 1–2 band (bottom) decays, the main band on the diagonal changes shape and shifts somewhat off the diagonal, and a new off-diagonal negative going peak appears (top). See text for details.

of the OD stretch is ~0.4 ps, although there is some wavelength dependence to the lifetime [3]. By $T_w = 450$ fs, a good fraction of the initially produced excited state population has decayed to the ground state. Therefore, by the time of the third pulse, the contribution to the signal from the diagram that gives rise to the 1–2 band is reduced. By $T_w = 1.2$ ps, the correlation spectrum has changed dramatically. The 1–2 off-diagonal peak is almost gone, and the diagonal δ band has clearly changed shape. A small band on the blue end of the diagonal 0–1 band has been uncovered. While the δ OD stretch has a lifetime of ~0.4 ps, the γ band has a lifetime of ~1 ps. As the δ band contracts to the red, the remnants of the γ band are uncovered. Most significant is the appearance of a new off-diagonal negative going peak located above the δ band. In the 1.8 ps plot, the 1–2 peak is gone. This is consistent with the ~0.4 ps vibrational lifetime. The positive going diagonal γ peak is almost gone, consistent with the ~1 ps lifetime. The diagonal δ band has contracted further to the red, and it has moved somewhat off of the diagonal. The shift of the position off of the diagonal is progressive; as T_w increases, the δ band contracts and shifts off of the diagonal. By 1.8 ps, the shift is quite pronounced. The new off-diagonal negative peak located above the δ band has grown considerably in magnitude. For $T_w = 5$ ps, the diagonal γ band is gone. The only remaining features are the δ band that is contracted to the red and shifted somewhat off of the diagonal and the off-diagonal negative going peak. Both peaks have broadened along the ω_τ axis. For times longer than ~5 ps, the peaks do not change shape significantly, but slowly decay in magnitude on a time scale of 10's of ps.

The T_w dependence of the correlation spectra raises a number of questions. First, why is there a δ band for times long compared to the vibrational lifetime? The 1–2 band decays with the lifetime, but the 0–1 band produces a strong signal for times much longer than the vibrational lifetime. Normally, decay of the excited state will cause the vibrational echo signal to vanish. Two rephasing diagrams contribute to the 0–1 signal. After the second interaction with the field (after the second pulse) one of these diagrams has a population in the excited state, the $v = 1$ level (diagram 1), and the other diagram has population in the ground state, the $v = 0$ level (diagram 0). The amplitudes of the populations oscillate as a function of frequency ω for a particular τ value as $1/2(1 + \cos(\omega\tau))$ for the $v = 1$ level and $-1/2(1 + \cos(\omega\tau))$ for the $v = 0$ level. These can be viewed as *frequency gratings* in the ground and excited states. The population peaks in the excited state correspond to population holes in the ground state. Vibrational relaxation causes the excited state grating to decay into the ground state, filling the ground state holes. Thus, the decay of diagram 1 into diagram 0 causes the signal to decay. Detailed experimental studies show that following vibrational relaxation, ~20% of the initially excited δs break on a very short time scale (~200 fs) [3]. Breaking a hydrogen bond attached to a δ removes it as a δ absorber. The broken bond destroys two δs and creates a γ and a β. Thus, the ground state *frequency grating* is not completely filled even following complete relaxation of the excited state. This leaves some amplitude in diagram 0. The third interaction with the field turns the ground state frequency grating into a 0–1 coherence and the signal is emitted. The ground state signal remains out to the hydrogen bond recombination time, which is 10's of ps [3].

The second question raised is what is the nature of the negative going off-diagonal peak that appears as T_w is increased? When hydrogen bonds attached to δs break, γs are formed. The newly formed γs give rise to an increase in the absorption in the γ region of the spectrum. The off-diagonal peak is composed of the products of hydrogen bond breaking. The peak is off diagonal because the first two interactions are with the δ band, but the third interaction is with the newly formed photoproduct γ band. The red shift along the ω_m axis of the newly formed γs with respect to the initially excited γs indicates the newly formed γs are not formed randomly within the γ band but are frequency correlated with the initially excited δs. The frequency correlation is also displayed in the T_w dependence of the dynamical line shape measured along the ω_τ axis. The frequency dimension, ω_τ, of the correlation spectra provides information that is not contained in other frequency and phase resolved techniques like frequency resolved IR

pump–probe. The extra dimension contains information about the frequency correlation between reactants and products through the dynamical line width measured as a function of T_w. This extra information allows us to consider two possible mechanisms that can give rise to the off-diagonal γ band signal. One contribution comes from non-rephasing grating diagrams. These give rise to signal when pulses 1 and 2 are within the free induction decay time of each other. An excited state *spatial grating* is formed. When this grating decays to the ground state and hydrogen bonds are broken, γs are produced having the same *spatial grating* pattern as the original excited state grating. The third pulse interacts with the γ *spatial grating* and produces a signal. The peak in the correlation spectrum, if generated by the grating diagrams, will have the full spectral line width along the ω_τ axis, and its dynamic line shape will be independent of T_w.

The other possible mechanism arises from rephasing diagrams and can occur for times τ greater than the free induction decay time. When the excited state *frequency grating* relaxes, hydrogen bonds are broken and γs are produced. If the newly formed γs are frequency correlated with their parent excited δs, then the ensemble of daughter γs will also form a *frequency grating*. The third pulse interacts with the γ *frequency grating* and produces a signal. Because the ground state *frequency grating* corresponds to a rephasing diagram, the observed dynamic line width can be narrower than the entire absorption line, and it can broaden because of spectral diffusion as T_w increases.

The important experimental observation is that the off-diagonal product γ peak broadens as T_w is increased from times greater than the lifetime to greater than 20 ps. As will be discussed in detail elsewhere [31], the observation of spectral diffusion in the off-diagonal product γ peak demonstrates that this peak has a substantial contribution from the ground state *frequency grating* rephasing diagram. Therefore, δ hydroxyl stretch vibrational relaxation produces product γs that are frequency correlated with the initially excited δs. The implication is that some of the degrees of freedom that determine the hydroxyl stretch frequency are not randomized by hydrogen bond breaking. These degrees of freedom of the local environment that, in part, determine the δ hydroxyl stretch frequency produce a frequency for the product γ that is correlated with the reactant δ.

The last question is, why does the δ band contract to the red and move off-diagonal as T_w becomes longer than the vibrational lifetime? The long-lived δ band exists because of hydrogen bond breaking that occurs following vibrational relaxation [3]. As time increases, the original δ band frequency gratings created by optical excitation across the entire δ band are replaced by the ground state frequency grating that is preserved by hydrogen bond breaking. The data indicate that hydrogen bonds on the red side of the δ band break more readily than those on the blue side. As will be discussed in detail subsequently, because of the large dynamical linewidth, the collapse of the band to the red also causes it to move off of the diagonal. The observed collapse of the band to the red is not influenced by the presence of the Fermi resonance. The identical behavior was observed in d-MeOD, which does not have the Fermi resonance.

The possibility that the collapse to the red of the δ band in the correlation spectrum is caused by preferential breaking of hydrogen bonds on the red side of the line is supported by two other experimental observations. Spectrally resolved pump–probe experiments display the analogous behavior. As time increases, the spectrum of the pump–probe signal narrows and shifts to the red. Furthermore, the temperature dependence of the linear absorption spectrum displays a shift to the blue of the δ band. As the temperature is increased, the equilibrium shifts so that there are fewer hydrogen bonds and those that remain are on average weaker. Preferential loss of hydrogen bonds on the red side of the line will produce the blue shift. This affect can be seen dramatically in temperature difference spectra [3]. These results are somewhat counter-intuitive. It is believed that hydrogen bonds on the red side of the line are stronger than those to the blue [22]. Nonetheless, the results indicate that vibrational relaxation preferentially breaks hydrogen bonds on the red side of the line.

If the dimension we Fourier transformed into the ω_τ axis is left in the time domain, it contains information similar to that obtained from three-pulse photon echo peak shift (3PEPS) measurements. 3PEPS is a popular method to describe dynamics for two-level systems where the decay of the shift can be directly related to the spectral diffusion in the system. More complicated systems such as hydrogen bonding in HDO in D_2O [32] and other reactive systems [33] exhibit more complicated echo peak shift behavior. We have measured the shift of the spectrally resolved echo at 2490 cm^{-1} as a function of T_w, shown in Fig. 4 (note log T_w scale). The peak shift displays behavior similar to behavior seen in other reactive systems [32,33]. Beginning at the shortest T_w, the peak shifts toward zero as spectral diffusion occurs, as expected. However, after several hundred fs, the peak shifts away from zero, reaching a maximum shift at ~1 ps. During this period, the system is undergoing the most dramatic population changes, as discussed above. For T_w delays longer than ~1 ps, the primary contribution to the echo signal at 2490 cm^{-1} is the residual δ band, which can be described as a two-level system. The peak shift decays with a 1.6 ps time constant, consistent with results obtained from time dependent IR hole burning experiments on MeOD [5], indicating that this decay is caused by spectral diffusion and not further population dynamics. By ~5 ps, the peak shift has reached its long-time offset value of about 20 fs. We are confident the offset is real because the phasing procedure is sensitive to <1 fs error in the time origin and chirp in our experiment. This procedure clearly indicates we set the time origin of the experiment to within 5 fs across the entire spectrum (>400 cm^{-1}).

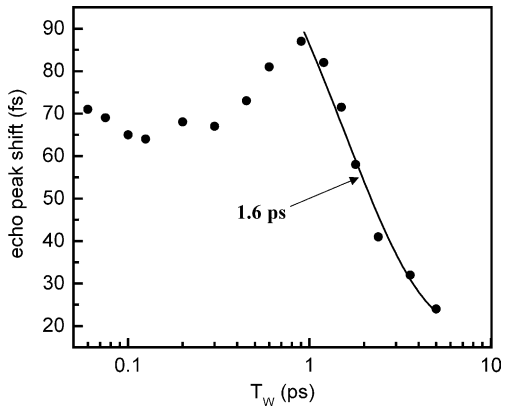

Fig. 4. Vibrational stimulated echo peak shift vs. T_w data for a cut through the 2D spectrum at 2490 cm^{-1}. (Note log T_w scale.) The peak shift reflects the extent of dynamical broadening. At long time the data decay exponentially with a time constant of 1.6 ps. For times short compared to the vibrational lifetime, the data are not monotonic (see text).

The non-zero offset of the peak shift suggests that static inhomogeneity exists in the residual δ band for longer than 10's of ps. As discussed above, the correlation spectra indicate the spectrum of the residual δ band narrows and is red-shifted relative to the δ band that is initially excited. The sample at room temperature is in the spectral diffusion regime and spectral diffusion occurs on a time scale slower than excited state relaxation of the δ band, [5] as seen in Fig. 4. Only the red δs that are preserved in the ground state contribute to the signal because the blue side of the band was not preserved through hydrogen bond breaking. This narrowing of the spectrum creates a type of static inhomogeneity that appears as though the red δs did not sample the whole band. The correlation spectra show that the δ band maintains the narrower spectrum for times longer than 10 ps. The non-zero offset of the peak shift displays this apparently static inhomogeneity. The description of the dynamics of spectral diffusion and pure dephasing must incorporate the population changes in order to adequately explain the system. These population changes cannot be discerned from the echo peak shift alone. Only by measuring the correlation spectra can we simultaneously obtain information about the spectral diffusion and populating dynamics and hence be able to separate them.

4. Concluding remarks

The results of ultrafast heterodyne detected multidimensional vibrational stimulated echoes with full phase information have been used to examine aspects of the hydrogen bond dynamics of methanol-OD in CCl_4. By using extremely short pulses (<50 fs), it is possible to excite the entire

very broad hydroxyl-stretching band including the 1–2 transition. A number of features that give rise to the data have been explicated. At short time, the correlation spectra are dominated by the hydrogen bonded OD stretch 0–1 transition (positive going peak) and the 1–2 transition (negative going peak). There is significant influence on the red side of 0–1 portion of the correlation spectrum from a Fermi resonance with the overtone of the methyl-rocking mode. This feature is absent in fully deuterated methanol.

The vibrational echo signal can be observed for times long compared to the vibrational lifetime (400 fs) because of the breaking of hydrogen bonds. As the hydrogen bonds break, the off-diagonal product γ peak grows in and broadens with time because of spectral diffusion. The results show that there is frequency correlation between the initially excited δs and the product γs. As T_w is increased beyond the vibrational lifetime, the broad diagonal δ band contracts to the red side of the line and shifts off of the diagonal. Hydrogen bond breaking following vibrational relaxation that occurs preferentially on the red side of the line can cause this behavior.

The types of experiments presented here give a greatly expanded picture of hydrogen bond dynamics. The full details of the experiments and data will be given in a subsequent publication. The equivalent experiments are currently underway on water.

Acknowledgements

This work was supported by the AFOSR (Grant No. F49620-01-1-0018), the National Institutes of Health (IR01-GM61137), the National Science Foundation (DMR-0088942), and the Department of Energy (Grant DE-FG03-84ER132SI). TS would like to thank the Alexander von Humboldt Foundation for partial support.

References

[1] H.-K. Nienhuys, S. Woutersen, R.A. van Santen, H.J. Bakker, J. Chem. Phys. 111 (1999) 1494.
[2] K. Gaffney, I. Piletic, M.D. Fayer, J. Phys. Chem. A 106 (2002) 9428.
[3] K.J. Gaffney, P.H. Davis, I.R. Piletic, N.E. Levinger, M.D. Fayer, J. Phys. Chem. A 106 (2002) 12012.
[4] K.J. Gaffney, I.R. Piletic, M.D. Fayer, J. Chem. Phys. 118 (2003) 2270.
[5] I.R. Piletic, K.J. Gaffney, M.D. Fayer, J. Chem. Phys. 119 (2003) in press.
[6] R. Laenen, G.M. Gale, N. Lascoux, J. Phys. Chem. A 103 (1999) 10708.
[7] G.M. Gale, G. Gallot, F. Hache, N. Lascoux, S. Bratos, J.C. Leicknam, Phys. Rev. Lett. 82 (1999) 1068.
[8] C.P. Lawrence, J.L. Skinner, J. Chem. Phys. 118 (2003) 264.
[9] A. Luzar, J. Chem. Phys. 113 (2000) 10663.
[10] R. Rey, K.B. Møller, J.T. Hynes, J. Phys. Chem. A 106 (2002) 11993.
[11] R. Veldhuizen, S.W. de Leeuw, J. Chem. Phys. 105 (1996) 2828.
[12] D. Zimdars, A. Tokmakoff, S. Chen, S.R. Greenfield, M.D. Fayer, T.I. Smith, H.A. Schwettman, Phys. Rev. Lett. 70 (1993) 2718.
[13] A. Tokmakoff, M.D. Fayer, J. Chem. Phys. 102 (1995) 2810.
[14] K.D. Rector, J.R. Engholm, C.W. Rella, J.R. Hill, D.D. Dlott, M.D. Fayer, J. Phys. Chem. A. 103 (1999) 2381.
[15] P. Hamm, M. Lim, R.M. Hochstrasser, Phys. Rev. Lett. 81 (1998) 5326.
[16] M.T. Zanni, M.C. Asplund, R.M. Hochstrasser, J. Chem. Phys. 114 (2001) 4579.
[17] K.A. Merchant, D.E. Thompson, M.D. Fayer, Phys. Rev. Lett. 86 (2001) 3899.
[18] O. Golonzka, M. Khalil, N. Demirdoven, A. Tokmakoff, Phys. Rev. Lett. 86 (2001) 2154.
[19] S.P. Yeremenko, S. Maxim, Wiersma, A. Douwe, Chem. Phys. Lett. 369 (2003) 107.
[20] R.R. Ernst, G. Bodenhausen, A. Wokaun, Nuclear Magnetic Resonance in One and Two Dimensions, Oxford University Press, Oxford, 1987.
[21] M.K.O. Golonzka, N. Demirdöven, A. Tokmakoff, Phys. Rev. Lett. 90 (2003) 047401.
[22] W. Mikenda, J. Mol. Struct. 147 (1986) 1.
[23] H. Graener, T.Q. Ye, A. Laubereau, J. Chem. Phys. 90 (1989) 3413.
[24] S. Woutersen, U. Emmerichs, H.J. Bakker, J. Chem. Phys. 107 (1997) 1483.
[25] C.P. Lawrence, J.L. Skinner, Chem. Phys. Lett. 369 (2003) 472.
[26] K.A. Merchant, D.E. Thompson, Q.-H. Xu, R.B. Williams, R.F. Loring, M.D. Fayer, Biophys. J. 82 (2002) 3277.
[27] S. Mukamel, Annu. Rev. Phys. Chem. 51 (2000) 691.
[28] H.N. Morita, Saburo, J. Mol. Spectr. 49 (1974) 401.
[29] J.E. Bertie, S.L. Zhang, J. Mol. Struct. 413–414 (1997) 333.

[30] V.M. Kenkre, A. Tokmakoff, M.D. Fayer, J. Chem. Phys. 101 (1994) 10618.
[31] J.B. Asbury, T. Steinel, C. Stromberg, K.J. Gaffney, I.R. Piletic, A. Goun, M.D. Fayer, J. Chem. Phys. (submitted).
[32] J.M. Stenger, D. Madsen, P. Hamm, E.T.J. Nibbering, T. Elsaesser, J. Phys. Chem. A 106 (2002) 2341.
[33] M. Yang, K. Ohta, G.R. Flemming, J. Chem. Phys. 110 (1999) 10243.